



Demand-Side Response for Grid-Independent Islands Based on Flexible Energy Management Using Heat Pumps

James Freeman^(✉), Daniel Coakley, and Charalampos Angelopoulos

Mitsubishi Electric R&D Centre Europe B.V., 17 Firth Road, Livingston EH54 5DJ,
United Kingdom

j.freeman@uk.merco.mee.com

Abstract. Large-scale deployment of local renewable energy sources (RES), coupled with demand-side response (DSR), is viewed as a critical strategy for improved energy security on geographic islands. This study, conducted as part of the Horizon 2020 “REACT” Project, focuses on the case-study island of Inishmore, western Ireland, under a future increased-renewables scenario in which the heating demand for 65% of the island’s 300 permanently-occupied off-gas grid dwellings is provided by air-to-water heat pumps. Simulations are performed using a community-scale energy system model, with the heat dynamics of the individual dwellings represented by reduced-order sub-component models. Rule-based control strategies are simulated for multiple DSR objectives, based on the concept of a centralised energy management platform issuing automated commands to each individual heat pump to serve as a dispatchable load. Annual simulation results presented in this paper include an 18% reduction in total renewable energy exported or curtailed under a “maximum RES self-consumption” strategy, and a 23% reduction in peak load under a “peak-load shifting” strategy.

Keywords: heat pumps · renewable energy · demand response · energy storage

1 Introduction

Demand-side response (DSR) is widely acknowledged as a future contributor to the decarbonisation of energy systems, with potential benefits for both grid operators, through improved management of electricity demand peaks, and for consumers through energy bill savings and other incentives in exchange for providing demand-side flexibility [1]. In the residential sector, recent years have seen the emergence of new opportunities for companies providing advanced home energy management services and offering savings through time-of-use (TOU) energy tariffs, optimisation of self-consumption, or grid flexibility services such as frequency response and virtual power plant (VPP) aggregation.

The electrification of heating and cooling demand using heat pump technology presents both advantages and disadvantages for supply and demand-side management. On the one hand, heat pumps can be driven by electricity from local renewable sources

such as wind and solar-PV, and can make use of low-temperature heat sources such as geothermal and the ambient air without the need to burn fuels directly. However, without effective energy management and storage, heat pumps could increase the required capacity of peaking power generation from non-intermittent (i.e. non-renewable) sources [2, 3].

REACT is a 4-year European project to address the challenges associated with DSR from the perspective of geographic islands with limited electrical grid access [4]. Islands face a number of challenges in terms of electrical grid infrastructure and are typically heavily reliant on energy imports, resulting in energy prices 100-400% higher than the mainland. Large-scale deployment of local renewable energy sources (RES) coupled with DSR on islands is viewed as a critical strategy for decarbonising energy systems under the *Clean Energy for EU Islands* initiative [5].

The key output of the REACT project is an adaptable cloud-based ICT platform for planning and management of RES and energy storage infrastructures to deliver cooperative energy management at the island community level. The technology will be demonstrated at three European pilot sites, one of which is the cluster of islands to the west of mainland Ireland known as the Aran Islands. Inishmore is the largest island in this cluster, with a permanent population of 760 inhabitants. The population can increase to > 1000 during the summer tourist season, during which time the mainland grid interconnection can come under severe strain.

Furthermore, the island is not served by a gas grid, and instead relies mainly on imported fuel oil from the mainland, at a significant cost to the local community. Recent years have seen an increased drive towards air-to-water (ATW) heat pumps as replacements for oil-fired boilers providing central heating and hot water. As a result, the demand for space heating and hot water increasingly affects the daily and seasonal profiles of electricity demand.

The project will demonstrate the REACT solution at a demo-site scale of 20-30 buildings, with a replication plan for uptake at the whole-island level. In this paper we use numerical simulation to assess the effectiveness of DSR with heat pumps when applied to a community of 200 dwellings (approximately 65% of the total number of permanently-occupied homes on Inishmore). The paper will focus on the technical implementation of possible control strategies, and thus the operation of the heat pump system is considered at a higher level of detail than other research efforts in this area. In particular, rule-based control strategies are simulated that realistically represent how commands issued in real-time by the demand-response platform can be implemented by the heat pump

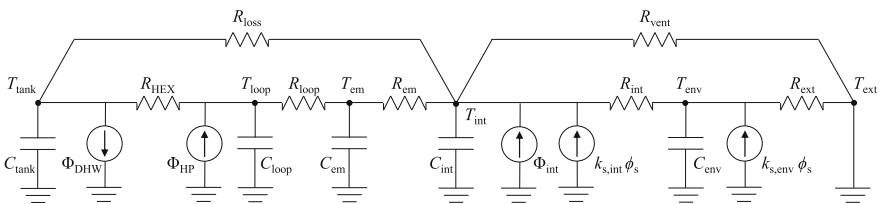


Fig. 1 Schematic R-C network representation of the reduced-order building thermal model

local controller to utilise the thermal storage potential of the domestic hot water (DHW) tanks.

2 Modelling Methodology

The island energy system model was implemented in MATLAB. The purpose of the model is to investigate the effectiveness of DSR control strategies at the community level over an annual period. The island community as defined within the model consists of 200 dwellings, each with an air-to-water (ATW) heat pump that serves as the main component for executing the DSR actions. Annual simulations are performed at a time resolution of 1-minute in order to capture the influence of short-duration demand events and their effect on the control actions of the heat pump systems. The model of the island energy system consists of the following components:

(i) the building thermal model; (ii) the heat pump controller sub-model; (iii) the renewable energy system (RES) model; and (iv) the demand-response control platform sub-model. In the following sections, an overview will be given of each of the sub-models and the main inputs described.

2.1 Building Sub-model

The building sub-model is used to simulate the demand for electrical and thermal energy based on a series of inputs including weather data, occupancy, and consumption profiles for electricity and hot water. Each building is represented by a network of lumped resistances and capacitances representing the thermal interactions of the major building components. Reduced-order resistance-capacitance (R-C) network models have been shown to be an effective approach for assessing the influence of the thermal dynamics of buildings on heating and cooling demand at the district level, and a number of configurations and approaches to calibration have been considered in previous works by Bacher and Madsen [6] and Aoun *et al.* [7].

The configuration adopted in the current work is summarised in Fig. 1, with the associated differential equations listed in Table 1. Each building consists of two nodes representing the respective thermal masses of the building envelope and internal space (with internal air volume and furnishings being lumped together as a single node). Additional nodes are included to represent the main components of the heating system; specifically, the primary circulation loop, DHW tank, and heat emitters are each represented by a single node in the thermal network model. Heat sources included in the model are solar gains (applied both to the envelope and directly to the internal space), internal gains from occupants and appliances, and the heat output delivered by the heat pump via the primary circulation loop.

Values for the R-C network model parameters are listed in Table 2, based on approximate geometry and construction information for a typical dwelling from the REACT project demo site on Inishmore: a detached single-storey bungalow, approximately 50 years old, with pumped cavity insulation, double-glazed windows and a floor area of 110 m². UA values denote rate of heat transfer per unit temperature difference and can be understood as the inverse of thermal resistance ($UA = 1/R$). Listed alongside in the table,

for comparison to the Inishmore dwelling, are experimentally-obtained values from a modern 3-bedroom house of similar total floor area at the Mitsubishi Electric test house facility in Livingston, Scotland, United Kingdom (for further details see Nguyen *et al.* [8]). In the present work, mean values of the thermal properties used in the simulation were based on the Inishmore dwelling. Each parameter was varied across the 200 buildings according to a normal distribution with a standard deviation of 5%. For input to the simulation, minute-resolution electricity and hot water demand profiles were generated for each building using free-to-use probabilistic tools [9, 10]. The demand profiles were calibrated by assuming year-round occupancy of 1-5 people per dwelling, with a mean occupancy of 2.3. Weather data for Inishmore was obtained from the NASA MERRA-2 service [11].

Table 1. Dynamic energy balance equations used in the reduced-order thermal model

$C_{\text{int}} \frac{dT_{\text{int}}}{dt} = UA_{\text{vent}} (T_{\text{ext}} - T_{\text{int}}) + UA_{\text{int}} (T_{\text{env}} - T_{\text{int}}) + UA_{\text{em}} (T_{\text{em}} - T_{\text{int}}) + k_{s,\text{int}} \phi_{\text{sol}} + \Phi_{\text{int}}$	(1)
$C_{\text{env}} \frac{dT_{\text{env}}}{dt} = UA_{\text{ext}} (T_{\text{ext}} - T_{\text{env}}) + UA_{\text{int}} (T_{\text{int}} - T_{\text{env}}) + k_{s,\text{env}} \phi_{\text{sol}}$	(2)
$C_{\text{em}} \frac{dT_{\text{em}}}{dt} = UA_{\text{loop}} (T_{\text{loop}} - T_{\text{em}}) + UA_{\text{em}} (T_{\text{int}} - T_{\text{em}})$	(3)
$C_{\text{tank}} \frac{dT_{\text{tank}}}{dt} = UA_{\text{HEX}} (T_{\text{loop}} - T_{\text{tank}}) + UA_{\text{loss}} (T_{\text{int}} - T_{\text{tank}}) + \Phi_{\text{DHW}}$	(4)
$C_{\text{loop}} \frac{dT_{\text{loop}}}{dt} = UA_{\text{HEX}} (T_{\text{tank}} - T_{\text{loop}}) + UA_{\text{loop}} (T_{\text{em}} - T_{\text{loop}}) + \Phi_{\text{ASHP}}$	(5)

Table 2. Building thermal properties

Parameter	Unit	Inishmore typical dwelling	Modern reference house
UA_{int}	W/K	240	95
UA_{ext}	W/K	2300	840
UA_{vent}	W/K	100	60
UA_{em}	W/K	400	150
UA_{loop}	W/K	1700	1700
UA_{HEX}	W/K	2700	2700
UA_{loss}	W/K	2.5	2.5
C_{int}	J/K	1×10^7	1×10^7
C_{env}	J/K	3×10^7	2.5×10^7
C_{em}	J/K	4×10^5	2×10^5
C_{loop}	J/K	2×10^5	2×10^5
$k_{s,\text{env}}$	m ²	8	8
$k_{s,\text{int}}$	m ²	1	1

Table 3. Default heat pump controller settings

Setting	Default value
DHW tank upper set point	50 °C
DHW tank lower set point	40 °C
DHW priority time limit	60 minutes
Legionella cycle temperature	65 °C
Legionella cycle duration	30 minutes
Legionella cycle frequency	15 days

2.2 Heat Pump Sub-model

Each building is assigned an ATW heat pump system for space heating (SH) and domestic hot water (DHW) provision. The heat pump operating characteristics are based on a Mitsubishi Electric Ecodan PUHZ-W85VAA with a 200-litre DHW tank and a nominal heating capacity of 8.5 kW. The heat pump supplies heat to a primary circulation water loop that flows through the heat emitters and also indirectly heats the DHW tank via a heat exchanger. Heat pump energy consumption as a function of outdoor air temperature and primary loop flow temperature is predicted using an efficiency curve derived from performance data published in the technical specifications [12].

Default settings for heat pump operation modes used in the baseline model are summarised in Table 3. DHW heating is activated when tank temperature drops below the lower set-point value, and stops when the tank temperature reaches the upper set-point, or when the time allowed for DHW heating is exceeded (if there is no demand for space heating in this time, DHW heating is allowed to continue). An important feature of the heat pump operation also included in the model is a regular legionella prevention (LP) cycle, in which the temperature of the tank is raised to a higher temperature to inhibit the growth of the legionella bacterium. Under default settings in the baseline model, the LP cycle is scheduled to occur once every fifteen days at a time of 3:00 AM. The operation of the heat pump in DSR mode is based on a configuration in which the heat pump local controller receives commands from the centralised demand-response platform. The platform also receives certain real-time operational information such as flow temperature, tank temperature and operation mode, made accessible by the heat pump's local controller. For Mitsubishi Electric heat pumps, such communication is currently possible via an API developer interface for the MELCloudTM cloud-based control system [13]. The commands issued by the demand response platform will be described further in Sect. 2.4

2.3 Renewable Energy System (RES) Sub-model

The renewable energy system sub-model consists of a hypothetical array of solar-PV panels and wind-turbines installed on the island. It is assumed that there is no electrical battery storage; the sizing of the solar and wind generators is performed according to a baseline simulation case with no demand-side response control, so that the annual

RES output is equal to the annual electricity demand for the cluster of buildings. This necessarily implies for the baseline case that self-sufficiency and self-consumption at the community level are equal, as defined in the following equations:

$$\text{Self-sufficiency} = 1 - \frac{E_{\text{imp}}}{E_{\text{dem}}} \quad (6)$$

$$\text{Self-consumption} = 1 - \frac{E_{\text{exp}}}{E_{\text{gen}}} \quad (7)$$

The relative installed capacities of solar and wind generation are then chosen to provide maximum self-sufficiency (and hence also maximum self-consumption) for the baseline case, with 25% solar and 75% wind found to be optimal. On this basis the PV array was sized at 2,320 m² assuming monocrystalline silicon panel properties, while the nominal installed wind capacity was 450 kW based on 2 × 225 kW_p turbines. Geographical positioning is not specified within the simplified model of the RES system, however it is assumed that there is no limitation in flexibility with which the electricity produced can be shared among the cluster of buildings.

In the simulation, the instantaneous electrical output from the PV array is calculated as a function of ambient temperature and solar irradiance according to PV panel nominal efficiency and temperature coefficient, assuming south-facing panels with an annually-optimal inclination angle of 37°. For the wind turbines, electrical output is calculated as a function of wind speed (corrected for hub height) according to the wind turbine's power curve and within the constraints of cut-in and cut-out limits. Wake effects of neighbouring turbines are not considered in the model. The electricity produced by the RES generators is distributed among the buildings according to instantaneous demand, with any surplus assumed to be exported to the mainland grid.

2.4 Demand-Response Platform Sub-model

The demand-response platform issues specific commands to the heat pumps based on the present state of the energy system. The DSR control actions in this work focus primarily on DHW mode, to make use of the operation time-shifting potential provided by the DHW storage tanks. At each time-step of the simulation, the platform monitors the status of the island energy grid and the potential for DSR based on the status of each heat pump and DHW tank. Two demand response modes are considered: (1) renewables self-consumption and (2) peak-load shifting.

2.4.1 Renewables Self-Consumption (RSC) Mode

In RSC mode, the demand-response platform seeks to match current grid demand with the availability of renewables generation. If there is a surplus of RES generation, the demand-response platform calculates the additional number of heat pumps to balance the surplus and issues individual "Forced DHW" commands, which the respective heat pumps respond to by charging their DHW tank to the upper temperature set-point. The rate at which heat pumps are activated is controlled, with priority given to heat pumps with the lowest tank temperature. To increase the storage potential, the upper tank temperature set-point is also raised from 50 °C to 60 °C during DSR operation.

2.4.2 Peak-Load Shifting (PLS) Mode

The objective of PLS mode is to even out the daily electricity consumption profile of the cluster of buildings through a combination of peak-shaving and valley-filling, to maximise the load factor over the daily period. The load factor is defined as the ratio of the average electrical load to the peak load:

$$\text{Load factor} = \frac{\bar{P}_e}{P_{e,\max}} \quad (8)$$

During times of low demand, the demand-response platform calculates the additional number of heat pumps to increase current consumption to the level of the previous 24-hour average. Idle heat pumps are brought online for DHW heating by issuing a “Forced DHW” command to those with the lowest tank temperature. As for the RSC mode, the upper tank temperature set-point is also raised to 60 °C and the rate of heat pump activation is moderated for stability.

3 Results

3.1 Baseline Case

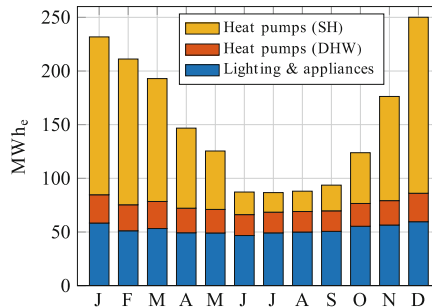
In the baseline case each heat pump provides SH and DHW according to the default heat pump controller settings. Over the annual period, 63% of the total electricity consumed is for the operation of the heat pumps. The monthly totals for electricity consumption and RES generation are shown in Fig. 2. A significant majority of the energy demand for space heating is in the winter months, while DHW consumption is more or less constant throughout the year. It is of note that more than three quarters of the annual heat pump consumption is for space heating, indicating that significant savings can potentially be achieved by addressing thermal losses from the buildings. By comparison, for the modern reference house the energy consumption for SH and DHW are approximately equal.

The electricity demand profile for a single day from the baseline simulation is shown in Fig. 3a. The background domestic electricity consumption for appliances and lighting, indicated by the blue area, is shown to peak in the evening hours (18:00–22:00), with a valley during the overnight period (00:00–07:00). The yellow and pink areas represent the electricity consumed by the heat pumps to provide space heating and DHW, respectively, in the 200 dwellings. A large spike can be observed at 8:00 due to the peak morning demand for hot water, which becomes the dominating feature of the total consumption profile. Smaller peaks in heat pump consumption are also observed at 3:30 and 13:00, with the former attributed to the night-time legionella cycle (occurring for 16 of the 200 heat pumps on the reference day plot), and the latter to a smaller lunchtime increase in hot water demand (Table 4).

The large morning spike in heat pump consumption occurs in response to the peak period of hot water demand occurring between 7:00–8:00. The heat map in Fig. 4a shows that during this period many of the hot water storage tanks in the 200 dwellings are depleted to below the 40 °C lower temperature limit at which the heat pump is triggered to operate. The sharp drop in tank temperature can be observed as a dark band

Table 4. Annual simulation results

	Baseline	RSC	PLS
Total demand, MWh _e	1814	1905	1889
HP demand (SH), MWh _e	917	876	882
HP demand (DHW), MWh _e	251	389	366
Grid Import, MWh _e	746	706	762
RES self-consumption (RSC)	59%	66%	62%
RES self-sufficiency (RSS)	59%	63%	60%
Days where RSS \geq 90%	93	115	92
Avg. daily load factor	48%	52%	65%
Avg. daily peak load, kW _e	421	409	324
Avg. heat pump COP	4.37	4.10	4.14
Avg. tank temp, °C	46.7	53.6	52.4
Avg. DHW cycles per year	754	1210	1077

**Fig. 2** Baseline case monthly consumption

on the heat map. Following this, it can also be observed that by 9:00 most tanks have been re-heated to their normal target temperature of 50 °C.

Without demand-side response, the electricity consumption generally shows a poor match with the available renewable energy generation (see Fig. 3a). RES generation capacity is sized to provide a total annual output equal to the total annual consumption in the baseline case, however due to the mis-match between the generation and demand profiles a total self-consumption of only 59% is achieved. For the reference day plot in Fig. 3a, RES generation peaks in the middle of the day due to the availability of solar irradiance, resulting in a surplus between 11:00–15:30. Meanwhile an average daily load factor of 48% demonstrates that the daily peak in electricity demand is on average more than double the daily mean.

3.2 Demand-Side Response Scenarios

3.2.1 Renewables Self-Consumption (RSC)

The renewables self-consumption case has the same installed RES generation capacity as the baseline case, but seeks to maximise the local self-consumption of renewables by improving the match between the load profile and the generation profile. By operating the heat pumps flexibly during periods of surplus generation to charge the DHW storage to an increased temperature, the total RES self-consumption is increased from 59% to 66% over the annual period.

From the perspective of the heat pump operation, the annual average DHW storage temperature increases from 46.7 °C in the baseline case to 53.6 °C in the RSC case, with the result that the average heat pump coefficient of performance (COP, defined as the ratio of the thermal energy output to the electrical energy input) drops by 6%. Thus a small increase in the total annual electricity demand is incurred, and as a result the RES self-sufficiency ratio increases from 59% to 63%; a smaller amount than the increase in RES self-consumption. The heat pumps are also required to run DHW heating cycles more frequently. Nonetheless, there is a 5% decrease in the net annual grid import, and a 24% increase in the number of days for which the RES is able to provide 90% or more of the local daily demand for electricity.

The modified demand profile in RSC mode can be compared to the baseline case in Fig. 3a, over the same 24-hour reference period. Figure 3b shows that for the RSC case, DSR mode is activated during the period of RES surplus between 11:00 and 15:30. The solid red line shows the number of additional heat pumps activated in order to raise the electricity demand and maximise self-consumption. Although the match between consumption and generation is visibly improved during this period, the effect on the consumption profile outside of the DSR-mode hours is relatively minor. In the evening hours, the heat pump energy consumption for DHW is significantly minimised, however the overall heat pump energy consumption is dominated by space heating. Due to the low availability of renewables in the early morning, little is achieved in terms of reducing the 8:00 peak in heat pump consumption for DHW. The smaller 3:00 peak in heat pump consumption observed in the baseline case is removed entirely in the RSC case by shifting the timing of the LP cycle to the early afternoon (14:30–15:00) when a surplus of renewables generation is more likely.

The utilisation of the storage potential in the DHW tanks can be examined in the heat map in Fig. 4b. It can be observed that by the end of the RES surplus period at 15:00, all of the DHW tanks for the 200 dwellings have been heated to the increased target temperature of 60 °C, while some tanks have been heated to an even higher temperature of 65 °C as a result of undergoing an LP cycle. Compared to the baseline case in Fig. 4a, there is little observable difference in tank temperatures during the early morning, prior to the peak DHW consumption period between 7:00–8:00.

3.2.2 Peak-Load Shifting (PLS)

The peak load shifting case seeks to flatten the energy consumption profile in line with the previous 24-h average. By running the heat pumps to charge the DHW tanks during hours of lower electricity demand, the average daily load factor is increased to 65%

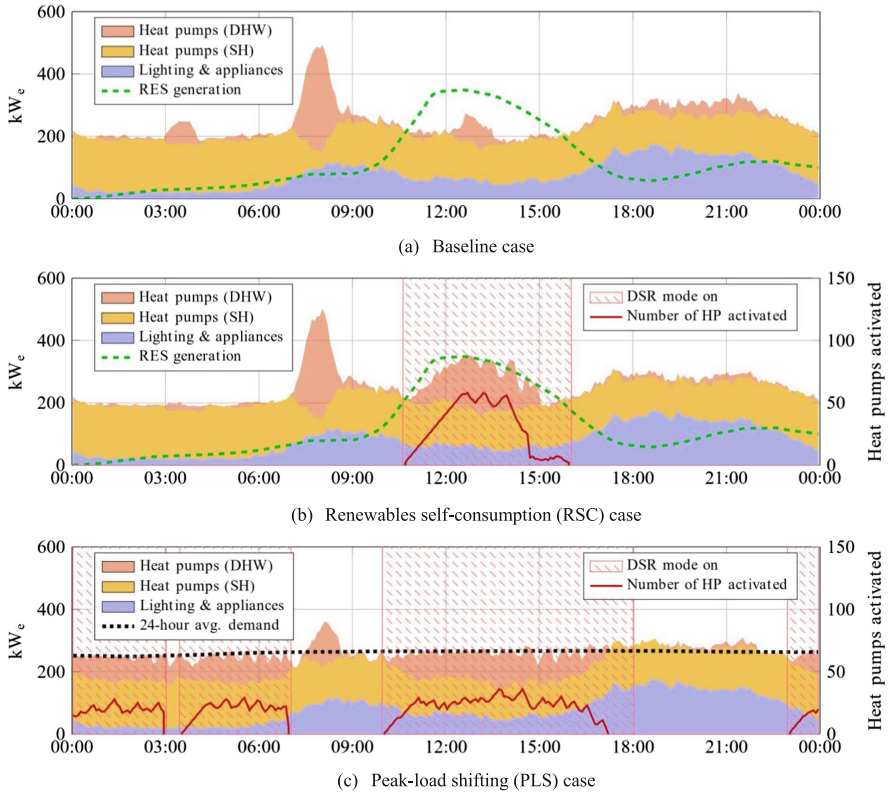


Fig. 3 Reference day (3rd February) energy consumption profiles

compared to the 48% in the baseline case; while the average daily peak load is reduced by 23%, from 421 kW to 324 kW.

As was the case for the RSC scenario, the increased tank temperature during the PLS mode results in a lower average heat pump COP and increases the total annual demand for electricity. Heat pumps are also required to perform a larger number of DHW heating cycles over the year, relative to the baseline. However, unlike the RSC case the net annual electricity import from the grid increases for PLS, because the heat pump operation is not controlled to maximise consumption during periods of surplus renewables generation.

The reference day electricity consumption profile for the PLS case is plotted in Fig. 3c. The solid red line shows that between 15–30 heat pumps are brought online simultaneously when DSR mode is active, raising the total consumption to the level of the previous 24-h average (~ 250 kW_e). This is also highly effective at reducing consumption during the high demand periods, in particular the 8:00 morning peak.

The heat map of the DHW tank temperatures in the PLS case is shown in Fig. 4c. By comparing this to the Baseline and RSC cases, it can be observed that far better use is made of the storage potential during the early morning hours to off-set the peak in heat pump operation that follows the peak in DHW demand. All tanks are charged to temperatures ≥ 60 °C before 7:00; with the result that fewer are fully depleted below

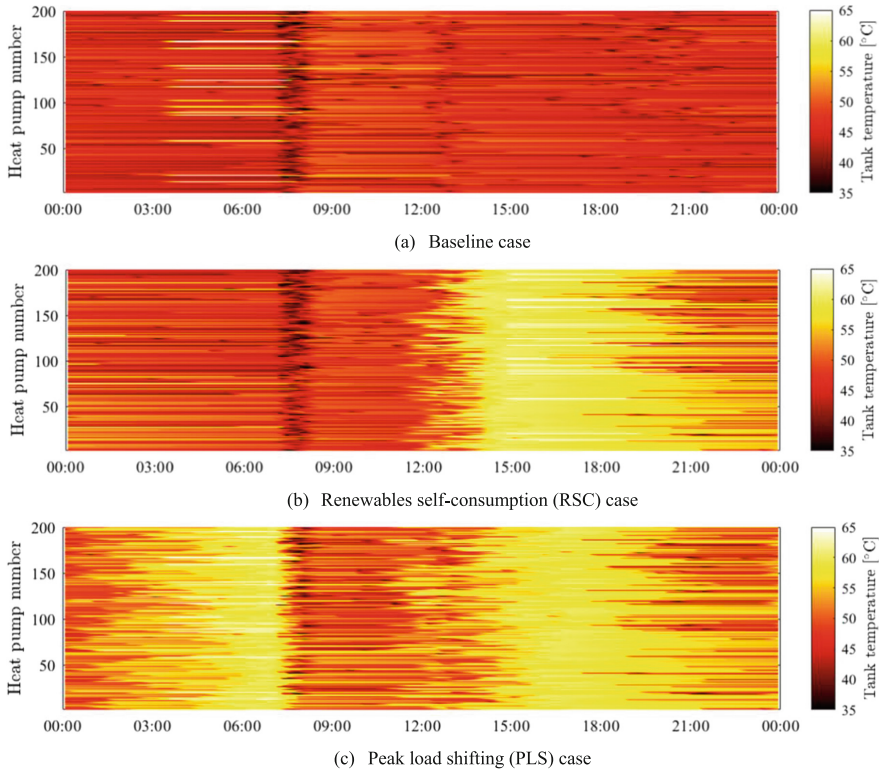


Fig. 4. Heat maps showing reference-day (3rd February) tank temperature profiles for the 200 dwellings

their lower temperature limit during the peak demand period and thus fewer heat pumps are triggered to run simultaneously in response.

4 Conclusions

In this paper, numerical simulation was used to assess the potential benefits of demand-side response on off-shore islands, based on domestic air-to-water heat pumps providing dispatchable load. The case study island of Inishmore was used, which is reliant on a connection to the Irish mainland grid for its electricity needs. A cluster of 200 dwellings with heat pumps was considered based on a future electrification of heat scenario, and demand-response strategies based on renewables self-consumption and peak-load shifting were investigated.

The simulation results have shown that the potential for energy savings through demand-side response is affected by several factors, including the daily and seasonal variations in the renewables generation profiles and heating demands of the buildings. Thermal storage using domestic hot water tanks offers a significant load-shifting potential for demand-side response, however for the typical Inishmore dwelling type considered in this work, space heating accounts for more than 75% of the heat pump energy

consumption. Electrification of heat demand results in a significant shift of seasonal electricity consumption to winter months, although the electricity base-load increase during the summer tourism period was not considered in the present study.

Nonetheless, this paper has demonstrated that a relatively simple form of rule-based control implemented within the demand-response platform can effectively manipulate the load profile of the cluster of heat pumps to achieve a 12% increase in renewables self-consumption or a 36% increase in average daily load factor. Future work in this area should consider the DSR benefits of thermal storage to offset large space heating loads, and advanced energy management approaches for RES shared self-consumption using combinations of thermal and electrical energy storage.

Acknowledgments. The authors wish to acknowledge valuable inputs from Duan Wu, Gordon McDonald, Conor Deane, Federico Seri, Peter O Donnacha and Cathy Ní Ghóill. This work was supported by funding from the European Union's Horizon 2020 research and innovation programme under grant agreement N° 824395.

References

1. T. Sweetnam, M. Fell, E. Oikonomou, T. Oreszczyn, Domestic demand-side response with heat pumps: controls and tariffs, *Building Research & Information* 47 (4), 2019, pp. 344–361.
2. C. Protopadaki, D. Saelens, Heat pump and PV impact on residential low-voltage distribution grids as a function of building and district properties, *Applied Energy* 192, 2017, pp. 268–281.
3. A. Arteconi, N.J. Hewitt, and F. Polonara, Domestic demand-side management (DSM): Role of heat pumps and thermal energy storage (TES) systems, *Applied Thermal Engineering*, 51 (1-2), 2013, pp. 155–165.
4. H2020: REACT. Renewable Energy for Self-sustainable Island Communities, 2019, <https://react2020.eu/>
5. European Commission, Clean energy for EU islands, 2017, https://ec.europa.eu/energy/topics/renewable-energy/initiatives-and-events/clean-energy-eu-islands_en
6. P. Bacher, and H. Madsen, Identifying suitable models for the heat dynamics of buildings, *Energy and Buildings* 43 (7), 2011, pp. 1511–1522.
7. N. Aoun, R. Baviere, M. Vallee, and G. Sandou, Development and assessment of a reduced-order building model designed for model predictive control of space-heating demand in district heating systems, *Proceedings of the 32nd International Conference on Efficiency, Cost, Optimization, Simulation and Environmental Impact of Energy Systems*, Wroclaw, Poland, 2019.
8. M. Nguyen, F. Baba, and A. Sung, Cold-soak testing method based evaluation of thermal performance of a typical residential dwelling, *Proceedings of the 4th International High Performance Buildings Conference*, Purdue University, USA, 2016.
9. I. Richardson, M. Thomson, Domestic electricity demand model V1.0. Loughborough University, 2010. <https://repository.lboro.ac.uk/ndownloader/files/17140067>
10. U. Jordan, K. Vajen, and H. Braas. DHWcalc V2.02b: Tool for the generation of domestic hot water (DHW) profiles on a statistical basis. University of Kassel, 2017. http://www.solare-prozesswarme.info/wp-content/uploads/2019/07/DHWcalc_2_02b.zip

11. NASA, Modern-Era Retrospective analysis for Research and Applications, Version 2 (MERRA-2), 2019, <https://gmao.gsfc.nasa.gov/reanalysis/MERRA-2/>
12. Mitsubishi Electric, Ecodan Data Book. Vol. 4.1, 2019, https://library.mitsubishielectric.co.uk/pdf/book/Ecodan_ATW_Databook_2019#page-1
13. Mitsubishi Electric, MELCloud User Manual, 2014, <https://www.melcloud.com/>

Open Access This chapter is licensed under the terms of the Creative Commons Attribution-NonCommercial 4.0 International License (<http://creativecommons.org/licenses/by-nc/4.0/>), which permits any noncommercial use, sharing, adaptation, distribution and reproduction in any medium or format, as long as you give appropriate credit to the original author(s) and the source, provide a link to the Creative Commons license and indicate if changes were made.

The images or other third party material in this chapter are included in the chapter's Creative Commons license, unless indicated otherwise in a credit line to the material. If material is not included in the chapter's Creative Commons license and your intended use is not permitted by statutory regulation or exceeds the permitted use, you will need to obtain permission directly from the copyright holder.

